

NAG-3955

N-34-CR

64694

P 7

## COMPUTATIONAL HEAT TRANSFER ANALYSIS FOR OSCILLATORY CHANNEL FLOWS

Mounir Ibrahim and Mohan Kannapareddy  
Mechanical Engineering Department, Cleveland State University,  
Cleveland, Ohio 44115, U.S.A.

### ABSTRACT

In this study an accurate finite-difference scheme has been utilized to investigate oscillatory, laminar and incompressible flow between two-parallel-plates and in circular tubes. The two-parallel-plates simulate the regenerator of a free-piston Stirling engine (foil type regenerator) and the channel wall was included in the analysis (conjugate heat transfer problem). The circular tubes simulate the cooler and heater of the engine with an isothermal wall. The study conducted covered a wide range for the maximum Reynolds number (from 75 to 60,000), Valensi number (from 2.5 to 700), and relative amplitude of fluid displacement (0.714 and 1.34).

The computational results indicate a complex nature of the heat flux distribution with time and axial location in the channel. At the channel mid-plane we observed two thermal cycles (out of phase with the flow) per each flow cycle. At this axial location the wall heat flux mean value, amplitude and phase shift with the flow are dependent upon the maximum Reynolds number, Valensi number and relative amplitude of fluid displacement. At other axial locations, the wall heat flux distribution is more complex.

### INTRODUCTION

Recently, a great deal of work has been devoted to study unsteady fluid flow and heat transfer both computationally and experimentally. In this paper attention is given to one particular class of unsteady flows namely oscillatory flow with zero mean input velocity. This is in contrast to other unsteady flows that have non-zero mean flow and known as "pulsatile flow".

One of the applications of oscillatory flow analyses is in the free-piston Stirling engine heat exchangers. In these engines the working fluid oscillates from the compression space to the expansion space going through the heat exchangers during the process. In this cyclic process the working fluid absorbs and releases energy within the various heat exchangers resulting in a net work output to the power piston. The design

codes modeling these type of engines currently use steady state correlations for estimating the friction and heat transfer losses.

In an oscillatory flow, the cyclic motion results in the velocity and temperature profiles being significantly different from those obtained from unidirectional or steady flows [1-3], which significantly effects the friction factor and heat transfer coefficient. Kurzweg [1] analytically solved the conjugate heat transfer problem for flow within two-parallel-plates channel, at the mid-plane of the channel (i.e. fully developed conditions). Kurzweg found that significant increase in the axial transport of heat can be achieved by flow oscillations without a significant mass transport between the hot and cold reservoirs. Similar analysis for circular tubes can be found in [4].

In this paper attention has been given to the engine heat exchangers namely: the 1) Regenerator, 2) Cooler, 3) Heater. The regenerator numerically modeled is the foil type which can be represented by a two-parallel-plates geometry (Ibrahim et al.[3]). Also, the cooler and heater are modeled as a single circular tube with constant wall temperature.

Figure 1 shows the envelope in which different Stirling engines operate, plotted in terms of the Valensi number ( $Va$ ) and maximum Reynolds number ( $Re_{max}$ ), and the cases investigated in this paper are also marked. The different criteria for transition from laminar to turbulent flow are shown by different straight lines [5,6]. For low  $Re_{max}$  (left side of the lines) the flow is laminar throughout the cycle; while for high  $Re_{max}$  (right side of these lines) the flow is a combination of laminar/transitional/turbulent over the cycle. As it is evident from the plot most of the Stirling engines operate in the transition or "fully turbulent" zone. Ahn and Ibrahim [7] tried to map the zones wherein quasi-steady turbulence models could be used for oscillating flow conditions, they used a High Reynolds Number turbulence model and found the predictions to be poor in the transition region. Recently an empirical transition model has been proposed for oscillatory flows [8], this model hopes to improve the predictions and is currently undergoing some testing.

Since computational turbulent or transitional flow conditions require experimental data for comparison (these data are not available today), the present study is restricted to laminar flow conditions.

## ANALYSIS

### Assumptions

Figure 2 shows the two geometries, with the inlet and boundary conditions examined in this paper. Figure 2a shows the conjugate problem where the channel wall is included in the computation domain. In this configuration the two-parallel-plates channel is used for code validation purpose as well as modelling the regenerator (foil type), of the Stirling engine (cases  $R_1$  &  $R_2$ ) employing the Cartesian coordinate system. Figure 2b shows the circular tube problem where the computation domain is limited to the fluid only, the tube wall being isothermal. This circular tube geometry is used to model the cooler (cases  $C_1$ ,  $C_2$  &  $C_3$ ) or the heater (cases  $H_1$ ,  $H_2$  &  $H_3$ ) of the Stirling engine employing the cylindrical coordinate system. The following assumptions are made: (1) the flow is laminar incompressible with constant thermophysical properties; (2) The inlet velocity profile is uniform but oscillating with time; (3) As for the heat transfer inlet and boundary conditions two cases are distinguished: i- (Cases  $R_1$  &  $R_2$ ) the fluid enters the channel with uniform temperature hot from one end and cold from the other end, maintaining uniform axial temperature gradient. The fluid exchanges heat with the solid wall which is subjected to the same uniform axial temperature gradient. ii- (Cases  $C_1$ ,  $C_2$ ,  $C_3$ ,  $H_1$ ,  $H_2$  &  $H_3$ ) the fluid enters the channel with uniform temperature and is heated (or cooled) by heat transfer from (or to) constant temperature walls; (4) The axial viscous diffusion as well as heat conduction are negligible.

### Mathematical Model

The system of partial differential equations in Cartesian and axisymmetric coordinate systems used to model the unsteady flow are as follows:

#### Continuity Equation:

$$\frac{\partial u}{\partial x} + \frac{1}{r^n} \frac{\partial}{\partial r}(r^n v) = 0 \quad (1)$$

$n=1$  for the axisymmetric coordinate system and,  
 $n=0$  for the Cartesian coordinate system with  $r=y$ .

#### Momentum Equations:

The conservation of momentum yields two scalar equations in the  $x$  and  $r$  directions respectively.

#### x-Momentum :

$$\rho \frac{\partial u}{\partial t} + \rho u \frac{\partial u}{\partial x} + \rho v \frac{\partial u}{\partial r} = -\frac{\partial P}{\partial x} + \frac{\partial}{\partial x}(\mu \frac{\partial u}{\partial x}) + \frac{1}{r^n} \frac{\partial}{\partial r}(r^n \mu \frac{\partial u}{\partial r}) + S_u \quad (2)$$

#### r-Momentum :

$$\rho \frac{\partial v}{\partial t} + \rho u \frac{\partial v}{\partial x} + \rho v \frac{\partial v}{\partial r} = -\frac{\partial P}{\partial r} + \frac{\partial}{\partial x}(\mu \frac{\partial v}{\partial x}) + \frac{1}{r^n} \frac{\partial}{\partial r}(r^n \mu \frac{\partial v}{\partial r}) + S_v \quad (3)$$

Here  $S_u$  and  $S_v$  denote the source terms in the momentum equations and are given as follows:

$$S_u = \frac{\partial}{\partial x}(\mu \frac{\partial u}{\partial x}) + \frac{1}{r^n} \frac{\partial}{\partial r}(r^n \mu \frac{\partial v}{\partial r}) \quad (4)$$

$$S_v = \frac{\partial}{\partial x}(\mu \frac{\partial v}{\partial r}) + \frac{1}{r^n} \frac{\partial}{\partial r}(r^n \mu \frac{\partial v}{\partial r}) - \left[ 2 \mu \frac{v}{r^2} \right] \cdot n \quad (5)$$

and  $P$  is the hydrodynamic pressure.

#### Energy Equation:

$$\rho \frac{\partial T}{\partial t} + \rho u \frac{\partial T}{\partial x} + \rho v \frac{\partial T}{\partial r} = \frac{\partial}{\partial x}(\frac{k}{c_p} \frac{\partial T}{\partial x}) + \frac{1}{r} \frac{\partial}{\partial r}(\frac{k}{c_p} \frac{\partial T}{\partial r}) + S_T \quad (6)$$

$S_T$  is the source term in the energy equation and is assumed to be zero or negligible in the paper.

#### Boundary Conditions:

The boundary conditions used to solve the above equations are:

a) At the walls:

$$u = v = 0 \text{ and } (T = T_{\text{wall}} \text{ OR } \dot{q}'' = \dot{q}''_{\text{wall}}) \quad (7)$$

b) At the axis of symmetry:

$$\frac{\partial u}{\partial r} = v = 0, \quad \dot{q}'' = 0 \quad (8)$$

c) Inlet plane:

$$u_{\text{in}} = u_{\text{max}} \sin(\omega t), \quad v_{\text{in}} = 0, \quad T_{\text{in}} = (T_{\text{cool/heater}}) \quad (9)$$

d) Outlet plane: Since the values of the dependent variables are not known a priori at these planes the gradients of the dependent variables in a direction normal to the outlet plane are neglected. Such a situation is valid if the outlet plane is far from the entrance or any recirculating activities.

$$\frac{\partial u}{\partial x} = \frac{\partial v}{\partial x} = \frac{\partial T}{\partial x} = 0 \quad (10)$$

## Numerical Method

The governing equations are solved numerically by a conservative finite volume (FV) method utilizing a modified version of the computer code CAST, developed by Peric and Scheureur [9]. The code has been extended to include time dependent boundary conditions (Oscillatory flows) and solve for conjugate heat transfer type problems. The system of linear algebraic equations for each conservative equations are solved by the efficient strongly implicit procedure (SIP) [10]. The nonlinear iterations are done by using the SIMPLE algorithm [11].

A 52x52 grid was used for all the cases investigated with grid density being high close to the walls and sparse away from it in the transverse direction, and a uniform grid was used in the longitudinal direction (axial). Convergence criteria was set at 0.1 % of the global residual norms for every dependent variable. For each case 120 time steps per cycle were used and at least 4 oscillation cycles were needed to reach quasi steady oscillating flow conditions. A typical run involved approximately 1000 seconds of CPU time per cycle on a Cray YMP/24 (sn 1040) supercomputer.

## RESULTS AND DISCUSSION

### CODE VALIDATION

Kurzweg [1] analytically solved the N-S equations governing the oscillatory flow between two-parallel-plates channel. The geometry investigated by him is shown in Fig. 2a. The flow is set to motion inside the channels by a sinusoidally varying pressure gradient, and a constant linear temperature gradient is maintained along the channel throughout the cycle. Kurzweg assumed the channels to be long such that the fluid flow is fully developed. Under this assumption the momentum equations simplify considerably and are tractable to analytical techniques.

In contrast to the analytical analysis, the numerical one has a two dimensional domain and finite; the flow is established by a sinusoidally varying velocity input  $[u_{in} = u_{max} \sin(\omega t)]$ , as it is, relatively, more difficult to apply pressure boundary conditions numerically. Figure 3 shows comparison between analytical and numerical velocity profiles at different velocity phase angles for the conjugate problem, case  $R_2$ :  $Re_{max} = 12000$  and  $Va = 400$  (see Table 1). The symbols are used for the analytical solution [1], while the dotted lines are used for the present work; the agreement between the two is excellent. Here the velocity profile shows the presence of a small Stokes layer (high Valensi number case) with the flow field is almost uniform in the channel core. At some instants the velocity profile exhibits a flow reversal near the wall.

Figure 4 shows comparison between analytical and numerical instantaneous temperature profiles  $(T - T_x)$  at different velocity phase angles for the conjugate problem, case  $R_2$ :  $Re_{max} = 12000$  and  $Va = 400$ . Here the temperature profile

shows a steep gradient near the wall and almost flat in the channel core with a possible maximum near the wall at some velocity phase angles. It should be noted that at some velocity phase angles (e.g. 90) the temperature in the core is almost similar to that at wall. Using conventional heat transfer relationship this will mean that the heat flux at the wall should be zero. However, the results indicate the presence of a temperature gradient at the wall and accordingly a heat transfer at the wall. As can be seen from the plots the agreement between the analytical and numerical results is excellent.

### Cooler and Heater Cases

Table 1 lists different cases investigated which cover a wide range of  $Re_{max}$ ,  $Va$  and  $A_r$ . These cases as well as others, were discussed in details in Kannapareddy [13]. In this paper, for the space limitations, we will present case  $H_2$  only.

Figure 5 shows the temperature contours at different velocity phase angles for the circular pipe problem and case  $H_2$

$Re_{max} = 16500$ ,  $Va = 88$ ,  $L/D_h = 70$  and  $A_r = 1.34$ . The contours are shown only for half of the cycle ( $0^\circ$  to  $180^\circ$ ) with cold fluid entering the tube (620 K) while keeping the wall at a hotter temperature (650 K). The entering fluid cold front advances into the channel during the acceleration portion of the cycle; this front continue advancing during the deceleration portion of the cycle but at a lower rate. Upon examining this case together with other cases we found that the velocity is out phase with the temperature; the degree of out phase is greater as the  $Re_{max}$  (or  $Va$ ) is higher. In contrast, as  $Re_{max}$  (or  $Va$ ) is very low (e.g. case  $R_1$ ) the velocity and temperature are in phase (not shown in this paper).

Figure 6 shows the normalized values for Nusselt number, wall heat flux and temperature difference at the channel axial mid-plane, for case  $H_2$ :  $Re_{max} = 16500$  and  $Va = 88$ . The temperature difference is obtained as the absolute difference between the wall and the section average fluid temperature on Fig. 6a and the bulk fluid temperature on Fig. 6b. On both figures the wall heat flux is the same, while the Nusselt number is different because of the temperature difference employed.

Using the section average temperature, the three quantities described above (Nusselt number, wall heat flux and temperature difference) are in phase with each other (Fig. 6a). On the other hand, using the bulk temperature [12], the temperature difference (and accordingly the Nusselt number) is out of phase with the heat flux (Fig. 6b). Moreover, the temperature difference passes through zero and accordingly, the Nusselt number shoots to infinity. It should be noted that the two plots show symmetry in time i.e. the thermal cycle is repeated twice for one flow cycle, this is due to the inflow symmetry and the plots are made at the channel mid-plane. At other planes this symmetry with time is lost as expected since the flow enters the channel at a uniform temperature.

Several other cases have been plotted (not shown in the paper) for other  $Re_{max}$ ,  $Va$  and  $A_r$ . These cases were plotted at different values of  $x/D_h$ . The plots reveal the complex nature of the heat flux distribution with time and axial location in the channel. Efforts are underway to Fourier analyze these results and try to obtain a heat transfer correlation of some practical use.

## CONCLUDING REMARKS

In this paper, we computationally examined the fluid flow and heat transfer in three different components of the Stirling engine namely regenerator, cooler and heater. Some of the cases examined are summarized in Table 1 and they represent the operating conditions of the NASA Space Power Demonstrator Engine.

Cases  $R_1$  and  $R_2$  resemble the regenerator and have been modeled using the conjugate heat transfer problem with a two-parallel-plate channel. Cases  $C_1$ ,  $C_2$  &  $C_3$  as well as  $H_1$ ,  $H_2$  &  $H_3$  resemble the cooler and heater respectively and have been modeled using the circular pipe with an isothermal wall.

The computational results revealed the following:

1- For low  $Re_{max}$  and (or)  $Va$ , the fluid flow and heat transfer for the regenerator (case  $R_1$ ) are quasi-steady i.e. the velocity and temperature profiles are parabolic. For high  $Re_{max}$  and (or)  $Va$  (case  $R_2$ ) flow reversal takes place near the wall at some parts of the cycle; also almost flat velocity and temperature profiles are obtained in the core of the channel. These cases were not only used for studying the foil type regenerator, but also to validate the code by comparing the computational results with analytical solution at similar operating conditions (the comparison showed excellent agreement).

2- The heat transfer results for the cooler and heater cases show that the heat transfer (in the channel mid-plane) goes through two cycles per each flow cycle. Also, the temperature profile is out of phase with the velocity profile particularly at the high  $Re_{max}$  and (or)  $Va$ .

3- The usual definition of the heat transfer coefficient in the case of oscillatory flows is ambiguous and limited due to the way the temperature difference is determined. The common practice has been to use the mixing cup or bulk temperature as the reference for the temperature difference as in the case of unidirectional or steady flows. But the bulk temperature definition (velocity weighted temperature across a cross section) breaks down in oscillatory flows due to flow reversal close to the wall for parts of the cycle at high  $Va$  and is especially true for laminar flows. A way of resolving this is to use the absolute value of the velocity in the definition of the bulk temperature and then evaluate the heat transfer coefficient. In this study both the section average temperature and bulk temperature were explored.

4- Using the section average temperature, the three quantities, namely, Nusselt number, wall heat flux and temperature difference are in phase with each other and out of phase with the flow. The wall heat flux is symmetric at 180 only in the mid-plane of the channel, other wise it has a different shape in the first half of the cycle compared with the second half. Also the wall heat maximizes at a lower velocity phase angle for larger  $A_r$  values (maximum wall heat flux in the mid-plane of the channel takes place at  $147^\circ$  for case  $C_2$  and at  $105^\circ$  for case  $H_2$ ).

5- On the other hand, using the bulk temperature, the temperature difference (and accordingly the Nusselt number) is out of phase with the heat flux (Fig. 6b). Moreover, the temperature difference passes through zero and accordingly, the Nusselt number shoots to infinity.

6- Several computational cases have been examined for other  $Re_{max}$ ,  $Va$  and  $A_r$  (not shown in the paper). The wall heat flux plots at different values of  $x/D_h$  reveal the complex nature of the heat flux distribution with time and axial location in the channel. Efforts are underway to Fourier analyze these results and try to obtain a heat transfer correlation of some practical use.

## ACKNOWLEDGEMENTS

This research has been conducted under NASA grant NAG3-955. Mr. Roy Tew, Jr. of NASA Lewis Research Center, Stirling Technology Branch, is greatly acknowledged for his valuable suggestions and encouragement throughout the course of this work.

## NOMENCLATURE

$a$	Half channel width in the conjugate problem.
$A_r$	Relative amplitude of fluid motion: $= (2X_{max}) / L$ $= \frac{1}{2} \cdot \frac{1}{(L/D_h)} \cdot \frac{Re_{max}}{Va}$
$b$	Half solid thickness in the conjugate problem.
$C_p$	Specific heat of the fluid or solid.
$D_h$	Hydraulic diameter of the tube or channel.
$k$	Thermal conductivity.
$L$	Length of the channel or tube.
$Nu$	Nusselts number.
$P$	Hydrodynamic pressure in the momentum equations.
$Pr$	Prandtl number of the fluid.
$\dot{q}''$	Heat flux.
$r$	Radial coordinate distance and direction for Axisymmetric cases or, the radius of the tube.

$Re_{max}$	Maximum Reynolds number: $= (\rho \cdot u_{max} \cdot D_h) / \mu$
$t$	Time [s].
$T$	Temperature in K. $T(x,y,t)$ or $T(x,r,t)$ .
$T_s$	Section averaged temperature of the fluid, $T_s(x,t) = [\int T r dr] / [\int r dr]$ .
$T_b$	Bulk temperature of the fluid weighted by the absolute velocity, $T_b(x,t) = [\int  u(r)  T r dr] / [\int  u(r)  r dr]$ .
$T_x$	Time averaged temperature, $T_x(x,y) = [T_{west} + \gamma x]$ .
$u$	Axial velocity in the x coordinate direction, $u(x,y,t)$ or $u(x,r,t)$ .
$u_{in}$	Axial velocity at the inlet, $u_{in}(t)$ .
$u_{max}$	Maximum input velocity in a cycle.
$v$	Normal velocity of the fluid in the y coordinate direction.
$Va$	Valensi Number: $Va = (\rho \cdot \omega \cdot D_h^2) / (4 \cdot \mu)$ .
$x$	Axial coordinate distance and direction.
$X_{max}$	Maximum amplitude of fluid displacement.
$y$	Normal coordinate distance and direction for Cartesian coordinate system.
<u>Greek:</u>	
$\omega$	Angular frequency in rad/sec.
$\mu$	Dynamic viscosity of the fluid.
$\gamma$	$= -(\partial T / \partial x) = [T_{west} - T_{east}] / L$ , time averaged constant axial temperature-gradient.
$\nu$	Kinematic viscosity of the fluid.
$\rho$	Density of the fluid.

## REFERENCES

1. Kurzweg, U. H. "Enhanced Heat Conduction in Oscillating Viscous Flows within Parallel-Plate Channels", Journal Of Fluid Mechanics, Vol. 156, pp. 291-300, 1985.
2. Simon, T.W. and Seume, J.R., "A Survey of Oscillating Flow in Stirling Engine Heat Exchangers", NASA Contractor Report 182108, March 1988.
3. Ibrahim, M. B., Tew, R. C. and Dudenhoefer, J. E. "Two Dimensional Numerical Simulation of a Stirling Engine Heat Exchanger", NASA Technical Memorandum 102057, 1989.
4. Kaviany, M. "Performance of a Heat Exchanger Based on Enhanced Heat Diffusion in Fluids by Oscillation: Analysis", Journal Of Heat Transfer, Vol. 112, pp. 49-55, February 1990.
5. Seume, J. R., "An Experimental Investigation of Transition in Oscillating Pipe Flow", Ph.D. Thesis, University of Minnesota, 1988.
6. Ohmi, M. and Iguchi, M. "Critical Reynolds Number in an Oscillating Pipe Flow" Bulletin of JSME, Vol. 25, No. 200, pp. 165-172, 1982.
7. Ahn, K-H. and Ibrahim, M. B. "Laminar/Turbulent Oscillating Flow in Circular Pipes", Int. J. Heat and Fluid Flow, Vol. 13, No. 4, pp. 340-346, December 1992.
8. Simon, T. W., Ibrahim, M. B., Kannapareddy, M., Johnson, T. and Friedman, G. "Transition of Oscillatory Flow in Tubes: An Empirical Model for Application to Stirling Engines", Proceedings of the 27th Intersociety Energy Conversion Engineering Conference, August 3-7, San Diego, CA, Vol. 5, pp. 495-502, 1992.
9. Peric, M. and Scheuerer, G. CAST-A Finite Volume Method for Predicting Two-Dimensional Flow and Heat Transfer Phenomena, GRS-Technische Notiz SSR-89-01, September 1989.
10. Stone, H. L. "Iterative Solution of Implicit Approximations of Multi-Dimensional Partial Differential Equations", SIAM J. Num. Anal., Vol. 5, pp. 530-558, 1968.
11. Patankar, S. V. and Spalding, D. B. "A Calculation Procedure for Heat, Mass and Momentum Transfer in Three-Dimensional Parabolic Flows", Int. J. Heat Mass Transfer, Vol. 15, p. 1787, 1972.
12. Patankar, S. V. and Oseid, K. "Numerical Prediction of the Heat Transfer in Transitional and Turbulent Oscillatory Flows", Progress Report submitted to Lewis Research Center, August 1992.
13. Kannapareddy, M., "Numerical Thermal Analysis of Heat Exchangers for the Stirling Engine Application", M.S. Thesis, Cleveland State University, 1993.

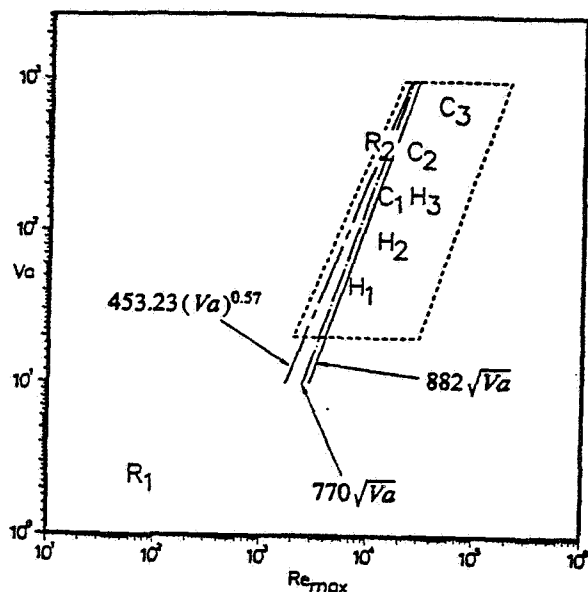


Figure 1 Envelope in which different Stirling Engines operate, together with:

- Criterion for transition from laminar to turbulent flow,
- Different cases studied in the present work.

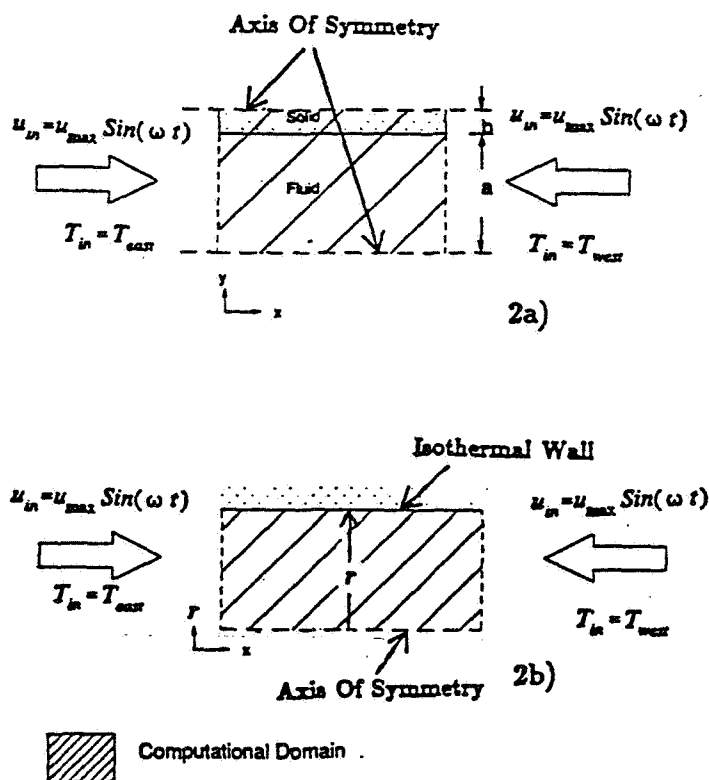


Figure 2 Different geometries, inlet and boundary conditions examined:

- Conjugate problem, flow between two parallel plates,
- Flow inside circular tube.

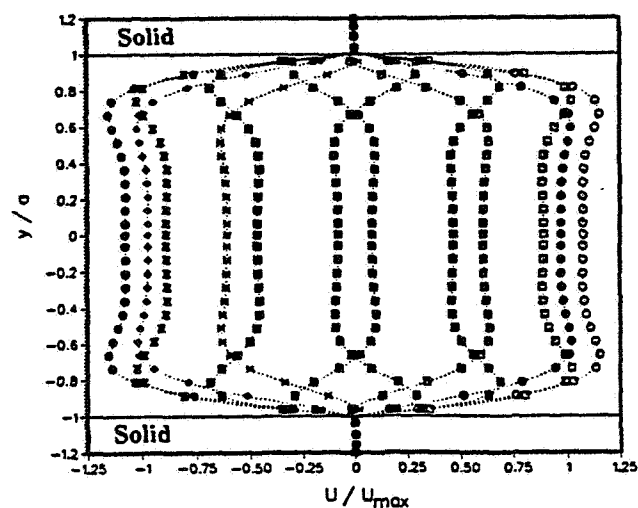


Figure 3 Comparison between analytical and numerical velocity profiles at different velocity phase angles for the conjugate problem for Case R<sub>2</sub>  $Re_{max} = 12000$  and  $Va = 400$ .

(Symbol : Analytical- Kurzweg [1]  
Dotted line : Numerical- Present work)

Velocity	■ = 30	● = 120	■ = 210	◆ = 300
Phase	□ = 60	□ = 150	■ = 240	× = 330
Angle	○ = 90	■ = 180	● = 270	■ = 360

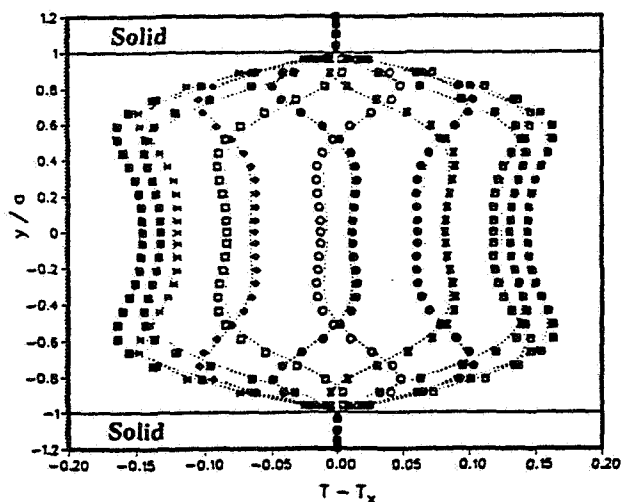


Figure 4 Comparison between analytical and numerical temperature profiles at different velocity phase angles for the conjugate problem for Case R<sub>2</sub>  $Re_{max} = 12000$  and  $Va = 400$ .

(Symbol : Analytical- Kurzweg [1]  
Dotted line : Numerical- Present work)

Velocity	■ = 30	● = 120	■ = 210	◆ = 300
Phase	□ = 60	□ = 150	■ = 240	× = 330
Angle	○ = 90	■ = 180	● = 270	■ = 360

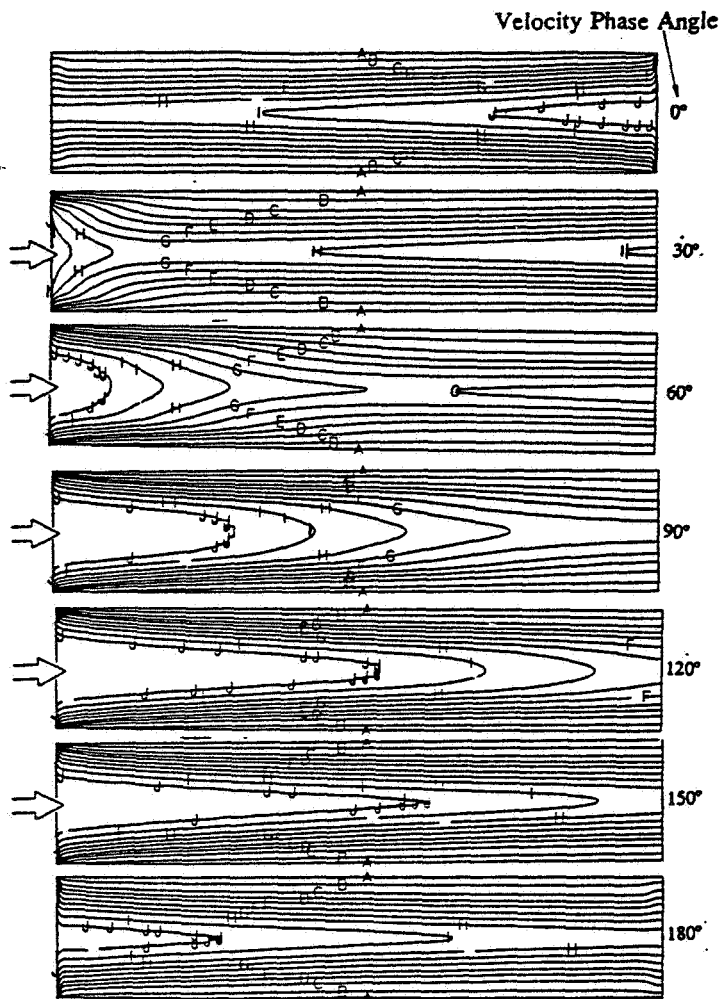
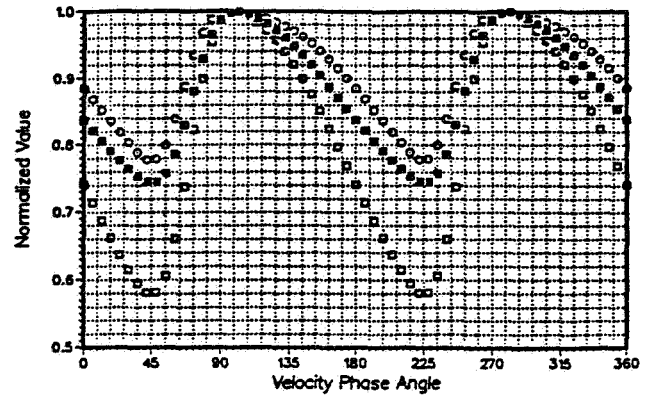


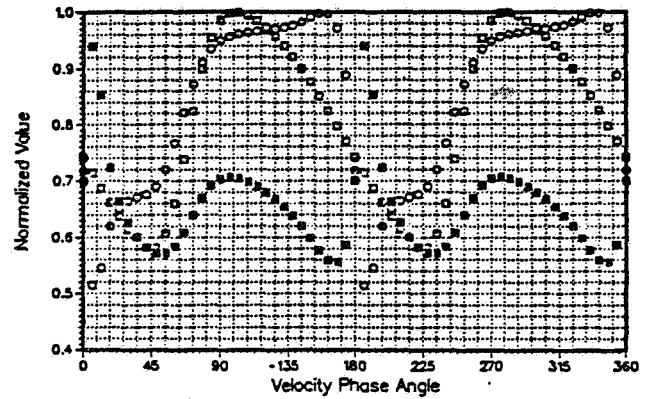
Figure 5 Temperature contours at different velocity phase angles for the circular pipe problem, Case  $H_2$   $Re_{max} = 16500$  and  $Va = 88$ .

[Temperature in K :

A:649.50, B:640.00, C:630.00, D:625.00, E:622.50  
 F:620.90, G:620.30, H:620.08, I:620.01, J:620.00]



6a) ■ =  $Nu/Nu_{max}$   
 □ =  $Q/Q_{max}$   
 ○ =  $(T_w - T_a)/(T_w - T_a)_{max}$



6b) ■ =  $Nu/Nu_{max}$   
 □ =  $Q/Q_{max}$   
 ○ =  $(T_b - T_w)/(T_b - T_w)_{max}$

Figure 6 Normalized values for Nusselt number, wall heat flux and temperature difference at the channel axial mid-plane, for Case  $H_2$   $Re_{max} = 16500$  and  $Va = 88$ , using:

a) Section average fluid temperature ( $T_a$ ).

b) Bulk fluid temperature ( $T_b$ ).